HIGHLY SENSITIVE POROUS SILICON SENSOR: DETECTION OF ORGANIC VAPOURS USING PHOTOLUMINESCENCE QUENCHING TECHNIQUE

Saakshi Dhanekar[1], S.S. Islam[1,*], T. Islam[1], Harsh[2]

[1]Nano-Sensor Research Laboratory, D/o Applied Science and Humanities,

Jamia Millia Islamia (Central University), New Delhi – 110025, India

[2]Solidstate Physics Laboratory (Defense Research & Development Organisation),

Teemarpur, Delhi – 110054, India

*Corresponding Author: safiul_el@rediffmail.com

Abstract- Porous silicon based sensors were tested in the presence of various linear aliphatic alcohols (methanol to n-hexanol) and water in the range of 10-100 ppm by photoluminescence quenching technique. An increasing trend in the degree of quenching was observed with the chain length of alcohols while minimum response was given to water. Sensitivity as high as 80-90% and nearly instant response time has proven the sensors to be highly efficient. Photoluminescence quenching phenomena is discussed on the basis of charge transfer mechanism between the host and the vapour-induced surface states, but the degree of quenching and anomalous response as a function of chain length suggests no unique quenching theory for estimating the sensitivity for the set of alcohols tested. From methanol to butanol, the sensitivity was dependent on the effective concentration of analytes in the porous silicon matrix, while for pentanol and hexanol having high boiling point, the sensitivity was linked to dielectric quenching mechanism due to the condensation of vapours inside the pores.

Index Terms: organic vapour, photoluminescence quenching, porous silicon, Raman, sensor

I. INTRODUCTION

Physical and optical properties of porous silicon (PS) have attracted much attention in the past few years [1,2]. The advantages of PS over its crystalline form include large surface to volume ratio, quantum confinement effects, ease of tuning bandgap for efficient light emission, and high sensing capabilities. Optical sensing has many advantages over electrical sensing like - no requirement of electrical contacts, safer to use in case of flammable gas or vapours, and more

interestingly, performance is directly linked to the pore morphology and surface species of the probe point [3]. The phenomenon of photoluminescence (PL) quenching effect in the presence of target analytes is used in optical sensing and has found a great scope since the last decade. A clear understanding of the interfacial electron, hole and energy transfer pathways accessible to PS is essential for optical sensor application purposes [4]. Many mechanisms for PL quenching have been discussed before [5-9] and some models were proposed listed as follows given in ref. [10]: (1) increase of non-radiative recombination rate in the nanoparticles due to alteration of the dielectric medium outside the Si nanocrystallites, (2) The enhancement of the non-radiative vibronic coupling to the surface vibrational modes, (3) The change of the nanoparticle surface electronic structure, and (4) The capture increase on the non-radiative traps at the forming of the strain-induced defects when molecules are adsorbed. Sensing by PL quenching mechanism has also been explained on the basis of energy transfer [11], charge transfer mechanism [12], vapour pressure [5], dielectric constant [13], dipole moment [14] of the molecules being adsorbed. Much work has been done for selectivity by PS based sensors [15]. However, the complete fact of PL quenching for such applications is still not understood.

In this work, the present authors have fabricated and tested highly sensitive PS based sensors with linear aliphatic alcohols (methanol to n-hexanol) and water. Sensitivity, response- and recovery time increased with the chain length of alcohols. Exceptional improvements in sensor response- and recovery time were observed for methanol, which is not reported so far. Sensing results are explained on the basis of vapour pressure, boiling point, and on the nature of organic molecule.

II. EXPERIMENTAL DETAILS

p-type PS samples of <100> orientation and 10Ω-cm resistivity were prepared by electrochemical anodization technique. Samples were etched in a 1:1 HF: ethanol solution in a current density 20 $mA.cm^{-2}$ for 40 mins. Pentane was used to dry the wet surface of PS as it reduces the capillary stress and prevents the surface cracking. The schematic diagram of the setup for PL quenching is shown in fig 1. It consists of a vapour chamber and a sensor chamber. The liquid organic solvent to be tested is converted into vapour phase by heating. The flow of dry nitrogen gas (carrier gas)

was fixed at 2L/min. Laser beam was directed onto the sensor through a confocal microscope and real time data was recorded through the spectrometer.

Figure 1. Raman Spectrometer and PL Quenching Setup

III. RESULTS AND DISCUSSIONS

Both the Raman and PL measurements of the samples were carried out by micro-Raman spectrophotometer (LabRAM HR800 JY) fitted with peltier cooled CCD detector and an Olympus BX-41 microscope. The excitation of the samples was performed with an air-cooled Ar^+ - laser (Spectra Physics) tuned at 488 nm. The spot size was 1.19 μm at sample surface under optimal conditions. Measurements were carried out in the back scattering geometry using a 50X LWD microscope objective. The laser power was kept low on the sample surface to avoid excessive heating.

The room temperature Raman spectra of PS is shown in figure 2. For the estimation of mean nanocrystallite size of the samples, the Raman data were analyzed within the framework of the phonon confinement model (PCM) developed by Richter et al [16] and Campbell et al [17].

The Raman bulk LO phonon peak (520 cm^{-1}) was found at 512.9 cm^{-1}. The model describes the Raman line shape of the optical phonons of low dimensional materials and has been widely

reported to estimate the nanocrystalline sizes [18,19]. The Raman intensity $I(\omega,L)$ in the phonon confinement model for a spherical nanocrystal with diameter L is given by

$$I(\omega,L)\alpha\int\frac{[C(q,L)]^2}{[\omega-\omega(q)]^2+(\Gamma/2)^2}d^3q \qquad (1)$$

where $\omega(q)$ is the phonon dispersion relation to the phonon momentum q, Γ is the natural linewidth of the bulk c-Si and $C(q,L)$ is the Fourier coefficient which gives the scattering probability of the phonons [18,19]. Considering the phonon weighing function to be Gaussian the Fourier coefficient for spherical crystallites is given by

$$[C(q,L)]^2=\exp(\frac{-q^2L^2}{4a^2}) \qquad (2)$$

The phonon dispersion relation ω(q) is given by

$$\omega(q)=\omega_0-120q^2 \qquad (3)$$

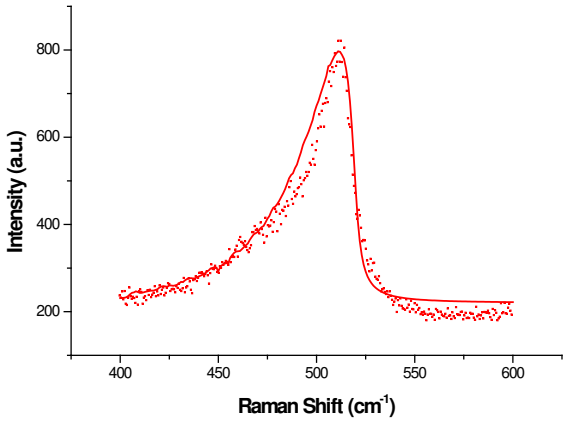

Figure 2. Raman spectral profile of the PS sample. Dotted lines show experimental data while smooth lines show fitting.

The estimated mean crystallite size, as obtained from the best fit to Fig. 2 is 4.8 nm.

The mean pore size was 50 nm as observed from SEM micrograph (Sigma, Zeiss) (figure 3). Many interconnected pores are visible in the SEM picture (encircled). The porosity of ~ 52% was calculated by gravimetric analysis.

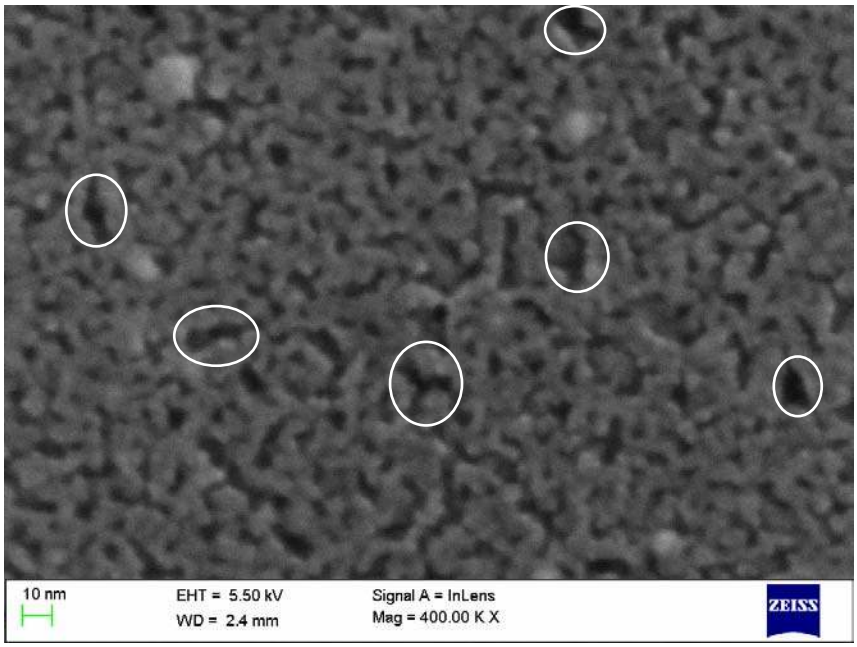

Figure 3. SEM image of sample showing the interconnection of pores

Figure 4 shows the PL spectra of the fabricated PS where the PL peak energy was observed at 1.72 eV for the as-anodized sample before quenching experiment was carried out. While exposing to organic vapours, it shows a decrease in intensity as well as small blueshift with the increase in vapour concentration. The quenching mechanism may be explained by charge transfer between the host (PS matrix) and the surface states created by vapour molecular species. PL takes place when electrons are absorbed from valence band (VB) to conduction band (CB) and a photon is emitted in the return journey. Photo-excited PS layer acts as electrons donor and vapour molecules act as acceptors as demonstrated in figure 5. The vapour molecules adsorbed on the PS surface restrict the recombination of electron and hole and thus PL quenching takes place. The blueshift in the PL spectrum also supports the charge transfer mechanism mediated by surface traps during adsorption and oxidation of molecules on the PS surface [9].

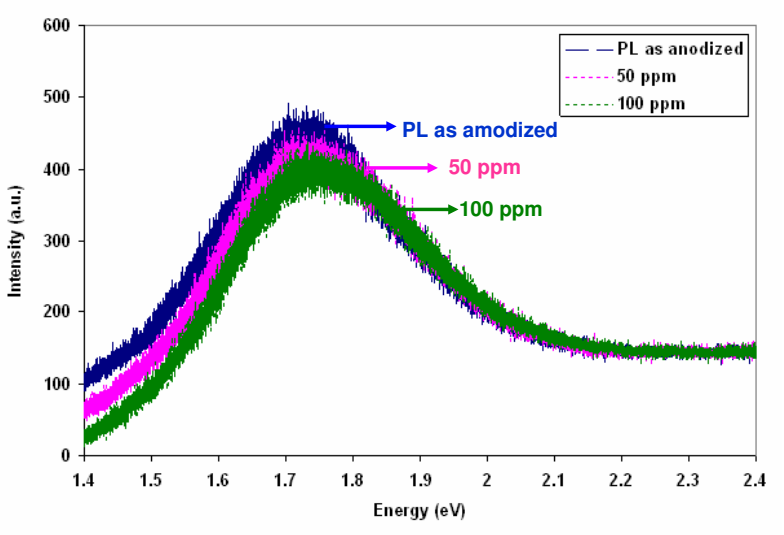

Figure 4. PL quenching with respect to energy at different concentrations of ethanol

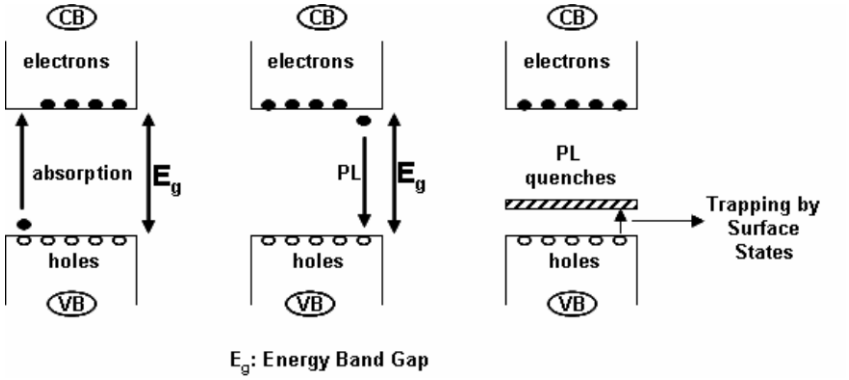

Figure 5.Simplfied form of explanation of PL quenching mechanism.

For sensing measurements, the samples were exposed to various linear aliphatic alcohols (methanol to n-hexanol) and water in the range of 10-100 ppm. When samples were tested by PL quenching technique during vapour injection-relaxation cycles, the PL peak (1.72 eV) was quenched and blue shifted. Figure 6 shows the real time testing of the sensor. PL quenching of the sensor tested with all alcohols at a fixed concentration of 25 ppm is shown in fig. 6(a)) and figure 6(b) shows the effect of quenching in presence of methanol and ethanol in a range of 10-100 ppm.

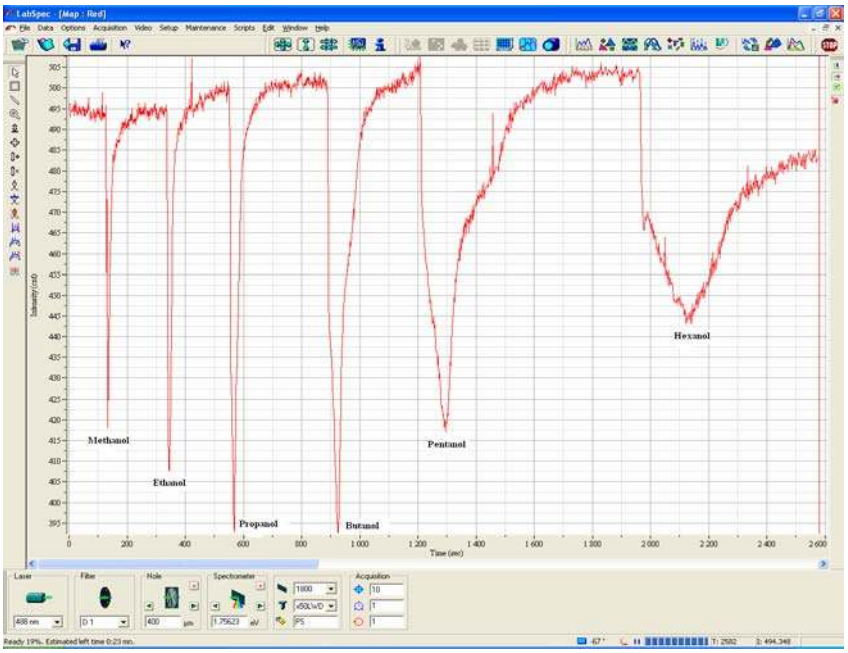

(a)

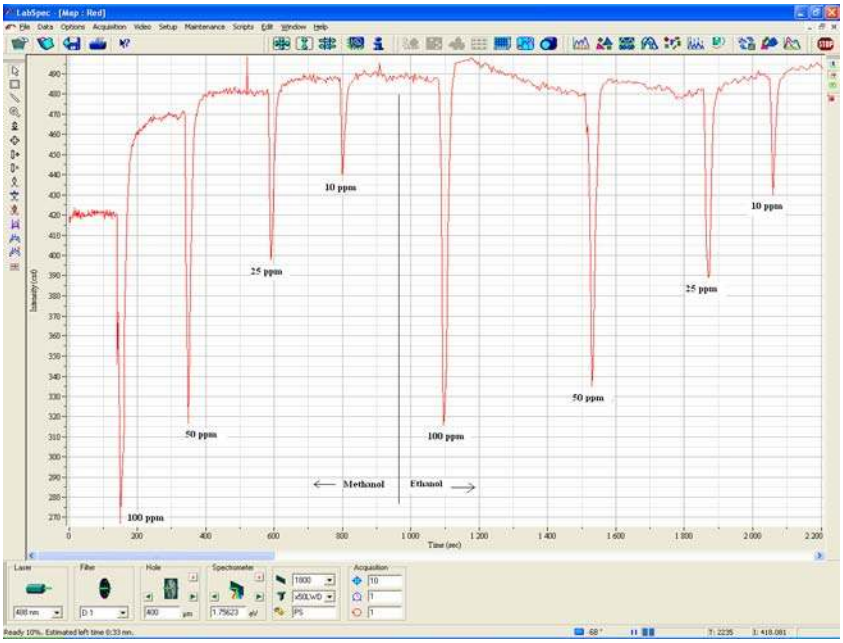

(b)

Figure 6. Real time testing of sensor (a) at 25 ppm with all linear aliphatic alcohols (methanol to n-hexanol), (b) with methanol and ethanol in a specified range of ppm.

The relative change in PL intensity of the sensors for different organic vapours is shown in figure 7(a), where I_0 and I are the intensities before and after quenching respectively. The slopes of these curves give the sensitivities of each organic vapour (fig 7(b)).

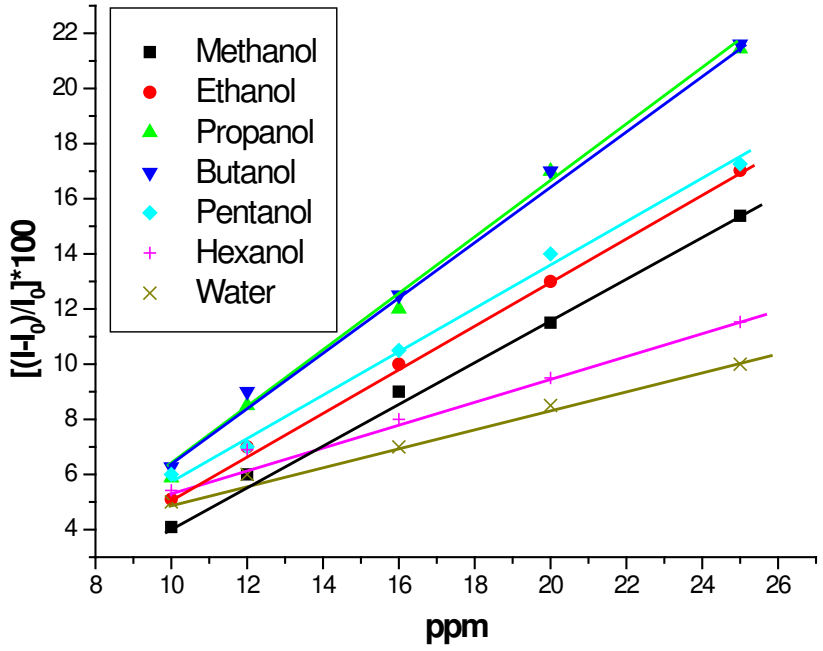

(a)

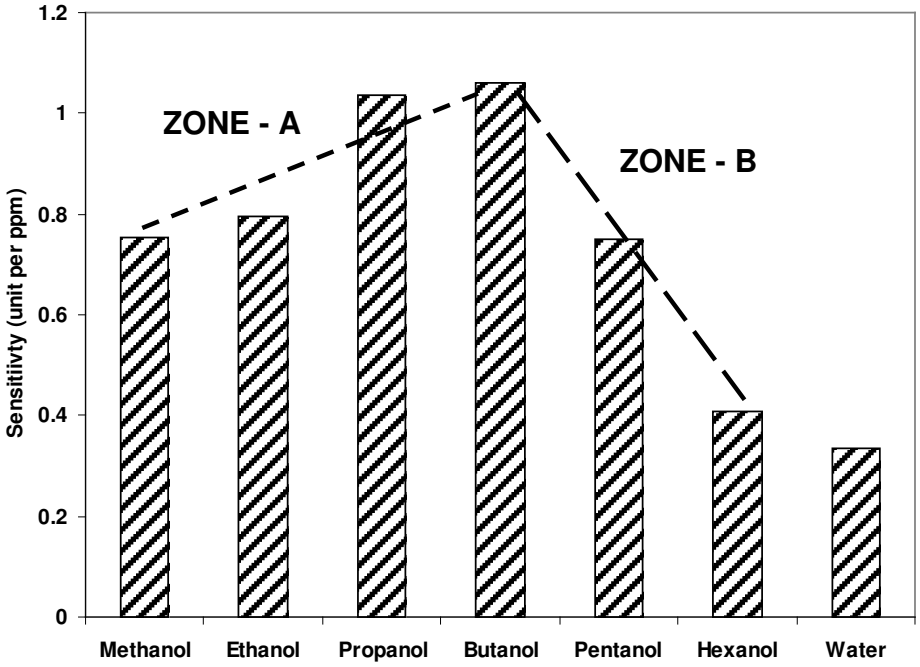

(b)

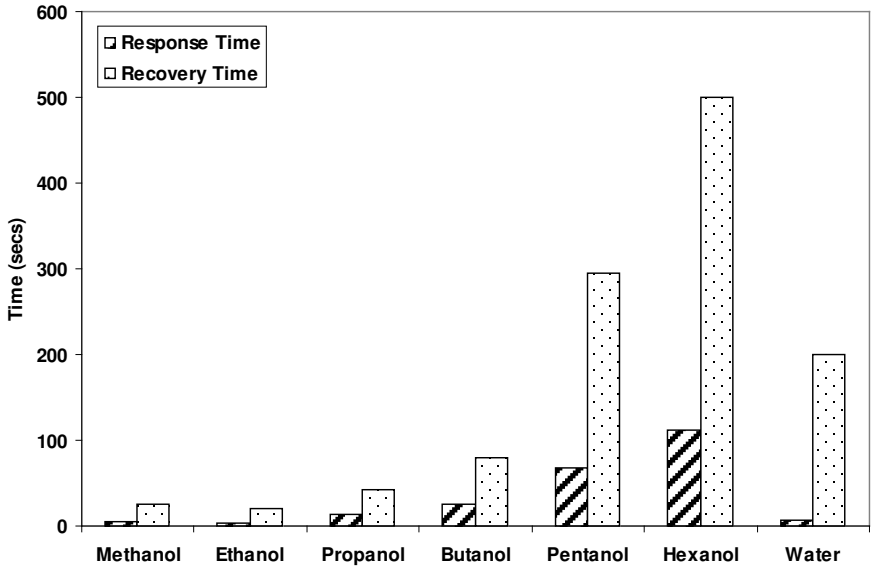

(c)

Figure 7(a) Response curve for all alcohols, (b) Sensitivity for all alcohols, (c) Comparison of response and recovery time for all alcohols.

Table 1: Physical properties of analytes tested [7]

Analyte	**Mol. Wt. (g/mol)**	**Dielectric Constant (at 25 °C)**	**Dipole (D)**	**Boiling Point (°C)**
Methanol	32.04	33	1.7	64.7
Ethanol	46.07	25.3	1.684	78.4
n- Propanol	60.1	20.8	1.55	97.1
n - Butanol	74.12	17.84	1.56	117.2
n - Pentanol	88.15	15.13	1.7	137.98
n - Hexanol	102.17	13.03	1.64	158
Water	18.02	80.2	1.861	100

Maximum sensitivity is observed for butanol amongst the vapour tested. As evident from fig.7(b) the sensitivity behavior may be divided into two zones – A and B. In zone-A, the sensitivity rises with chain length (upto butanol) whereas an opposite trend is observed for pentanol and hexanol

in zone-B. Researchers have found that in case of alcohols in vapour phase, the sensitivity is primarily dependent on the concentration of vapour in the PS matrix and it should increase with the chain length [5,6]. But, it is clear from fig.7(b) that a single quenching mechanism may not be applicable for all the linear aliphatic alcohols (methanol to hexanol).

Dian et al [7] have proposed that the alcohols in vapour phase interact with PS matrix and their effective concentration inside the pores is determined by capillary condensation effect [20]; the lower is the saturated vapour pressure inside the pores, higher is the analyte concentration in PS matrix [7]. As chain length of alcohol increases, vapour pressure inside the pores decreases and therefore more vapours may condense in the pores leading to higher sensitivity. Our results are in good agreement with the said approach. But this does not conform as shown in case of zone-B.

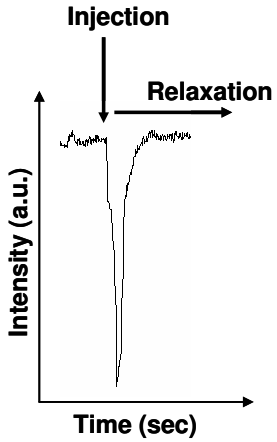

Figure 8. Response curve of one of the alcohols showing the injection and relaxation profiles

This may be interpreted as follows. Pentanol and hexanol have higher boiling points in comparison to other alcohols of lower chain length (Table 1). As a result, the saturated vapour pressure inside the pores becomes extremely low vis-à-vis the molecules in zone-A; therefore, the vapour condensation leading to a phase transformation from vapour to liquid inside the pores is highly probable. This causes a decrease in sensitivity as the dependency on vapour phase has ended and instead dielectric quenching mechanism as proposed by Dian et. al. [7], plays a dominant role for sensing. This results in a slow recovery and broadening of the injection-relaxation profile as shown in fig 8. .Therefore, we assume that molecules in zone-B do not remain in vapour phase after infiltration inside the pores and it needs further studies for alcohols of much higher chain lengths. The response of water was observed to be insignificant in

comparison to various alcohols. Thus it may be concluded that sensitivity is dependent neither on one theory nor on the trend of any of the physical parameters given in table 1.

The other sensor parameters like response- and recovery time were also calculated for the sensors. The results are depicted in fig 7(c). Both the response- and recovery time were found to increase with the chain length. However, our sensors have shown almost instant response (in few seconds) for methanol, in contrast to the results reported so far [5]. A minimum response- and recovery time of 5 and 25 sec respectively was observed for methanol and a maximum of 112 and 500 sec for hexanol. High response time shows slow adsorption of molecule on the pores of porous structure of silicon. This may be due to the fact that with the increase in chain length, the molecular structure becomes more bulky restricting quick adsorption into the nanopores of silicon. Also, the boiling point increases with chain length that does not allow the condensed molecules to get desorbed easily from the pores causing a rise in recovery time. This justifies the broadening of response curve with increasing chain length.

IV. CONCLUSION

The PS samples prepared by electrochemical anodization technique were tested for linear aliphatic alcohols (methanol to n-hexanol) and water. Not much response was given to water; and among the alcohols tested, butanol had shown maximum sensitivity. Two separate theories were followed during PL quenching for the entire set of alcohols. From methanol to butanol, the saturated vapour pressure of the molecules inside the pores play an important role for increasing sensitivity, whereas phase transformation from vapour to liquid takes place in case of pentanol and hexanol as the dependency on vapour phase had ended and instead dielectric quenching mechanism dominated. Response- and recovery time had shown an increasing trend with an increase in chain length of alcohol. Instantaneous response time was observed for methanol and its quite competitive sensitivity with respect to butanol had proven the sensors to be highly efficient. This study may open the possibility for commercialization of such type of optical sensors.

V. ACKNOWLEDGEMENT

The authors[1] gratefully acknowledge the financial support provided by Ministry of Communication & Information Technology, Govt. of India, through its Grant No. Nano (9), 2006.

REFERENCES

[1] A.T. Fiory and N.M. Ravindra, "Light emission from silicon: Some perspectives and applications", Journal of Electronic Materials, vol. 32, issue 10, pp. 1043-1051, 2003.

[2] N. Chi, D.L. Phillips and K. Chan, "In situ photoluminescence characterization of porous silicon formation", Thin Solid Films, vol. 342, pp. 142-147, 1999.

[3] V. Mulloni, L. Pavesi, "Porous microcavities as optical chemical sensors", Applied Physics Letters, vol. 76, pp. 2523-2525, 2000.

[4] D. L. Fischer, J. Harper, M. J. Sailor, "Energy transfer of porous silicon photoluminescence by aromatic molecules", Journal of American Chemical Society, vol. 117, pp. 7846-7847, 1995.

[5] T. Chvojka, V. Vrkoslav, I. Jelínek, J.Jindřich, M. Lorenc, J.Dian, "Mechanisms of photoluminescence sensor response of porous silicon for organic species in gas and liquid phases", Sensors and Actuator B, vol. 100, pp. 246-249, 2004.

[6] J. Dian, V. Vrkoslav, I. Jelínek, "Chemical sensing by simultaneous measurement of photoluminescence decay time of porous silicon", Phys. Status Solidi (c), vol. 4, pp. 2078-2082, 2007.

[7] J. Dian, T.Chvojka, V. Vrkoslav, I. Jelínek, "Photoluminescence quenching of porous silicon in gas and liquid phases – the role of dielectric quenching and capillary condensation effects", Phys. Status Solidi (c), vol. 2, pp. 3481-3485, 2005.

[8] W.J. Jin, G. L .Shen, R.Q. Yu, "Organic solvent induced quenching of porous silicon photoluminescence", Spectrochimica Acta Part A, vol. 54, pp. 1407-141, 1998.

[9] W.J. Salcedo, F.J.R. Fernandez, J.C.Rubim, "Photoluminescence quenching effect on porous silicon films for gas sensors application", Spectrochimica Acta A, vol. 60, pp. 1065-1070, 2004.

[10] V.A. Skryshevsky, "Photoluminescence of inhomogenous porous silicon at gas adsorption", Applied Surface Science, vol. 157, pp. 145-150, 2000.

[11] J. Harper, M.J. Sailor, "Photoluminescence quenching and the photochemical oxidation of porous silicon by molecular oxygen", Langmuir, vol. 13, pp. 4652-4658, 1997.

[12] D. R. Striplin, C. G. Wall, B.W. Erickson, T. J. Meyer, “Energy Transfer from Luminescent Porous Silicon to Adsorbed Osmium(II) and Ruthenium(II) Polypyridyl Complexes”, Journal Physical Chemistry B, vol. 102, pp. 2383-2390, 1998.

[13] S. Fellah, R. B. Wehrspohn, N. Gabouze, F. Ozanam, J.-N. Chazalviel , “PL quenching of porous silicon in organic solvents: evidence for dielectric effects”, Journal of Luminescence, vol. 80, pp. 109-113, 1999.

[14] J. M. Lauerhaas, Grace M. Credo, J. L. Heinrich, and M. J. Sailor, “Reversible Luminescence Quenching of Porous Si by Solvents”, Journal of American Chemical Society, vol. 114, pp. 1911-1912, 1992.

[15] L. Zhang, J. L. Coffer, J. Wang, C. D. Gutsche, “Porous Silicon Coated with Calixarene Carboxylic Acid Derivatives: Effects on Luminescence Quenching Selectivity”, Journal of American Chemical Society, vol. 18, pp. 12840-12841, 1996.

[16] H. Richter, Z. P. Wang, L. Ley, “The one phonon Raman spectrum in microcrystalline silicon”, Solid State Communications”, vol. 39, pp. 625-29, 1981.

[17] I. H. Campbell, P. M. Fauchet, “The effects of microcrystal size and shape on the phonon Raman spectra of crystalline semiconductors”, Solid State Communications, vol. 58, pp. 739-741, 1986.

[18] Md. N. Islam, A. Pradhan, S. Kumar, "Effects of crystallite size distribution on the Raman- scattering profiles of silicon nanostructures", Journal of Applied Physics, vol. 98, pp. 0234309, 2005.

[19] M. Yang, D. Huang, P. Hao, F. Zhang, x. Hou, X. Wang, "Study of the raman peak shift and the linewidth of light emitting porous silicon", Journal of Applied Physics, vol. 75, pp. 651-653, 1994.

[20] S. J. Gregg, K. S. W. Singh, Adsorption, Surface Area and Porosity, Academic Press, London, 1967.